TISSUE ENGINEERING: Part A
Volume 16, Number 2, 2010

DOI: 10.1089/ten.tea.2009.0426

Vascular Endothelial Growth Factor Inhibits Bone Morphogenetic Protein 2 Expression in Rat Mesenchymal Stem Cells

Björn H. Schönmeyr, M.D., Marc Soares, M.D., Tomer Avraham, M.D., Nicholas W. Clavin, M.D., Fredrik Gewalli, M.D., Ph.D., and Babak J. Mehrara, M.D., FACS

Introduction: While several studies report that bone morphogenetic proteins (*BMPs*) and vascular endothelial growth factor (*VEGF*) can act synergistically to improve bone tissue engineering, others suggest that VEGF inhibits osteogenesis. The purpose of these experiments was therefore to evaluate the effect of dual transfection of these growth factors and potential mechanisms of interaction on gene expression and osteogenesis *in vitro* and *in vivo*. *Methods:* Marrow-derived mesenchymal stem cells (MSCs) were exposed to recombinant *VEGF* protein or transfected with adenoviruses encoding *BMP2*, *VEGF*, or *LacZ* in a variety of ratios. Alterations in gene and protein expression *in vitro* as well as bone formation *in vivo* were assessed. *Results:* MSC exposure to AdV-VEGF or recombinant *VEGF* inhibited *BMP2* mRNA expression, protein production, and MSC differentiation. Co-culture experiments revealed that BMP2 suppression occurs through both an autocrine and a paracrine mechanism, occurring at the transcriptional level. Compared to controls, cotransfection of *VEGF* and *BMP2* transgenes prevented ectopic bone formation *in vivo*. *Conclusion: VEGF* is a potent inhibitor of *BMP2* expression in MSCs, and supplementation or overexpression of *VEGF* inhibits osteogenesis *in vitro* and ectopic bone formation *in vivo.* Strategies to utilize MSCs in bone tissue engineering therefore require careful optimization and precise delivery of growth factors for maximal bone formation.

Introduction

Mesenchymal stem cells (MSCs) are pluripotential adult stem cells that can be isolated from a number of different tissues, including bone marrow, skin, and fat. These cells are easily isolated and can be culture expanded. Culturing the cells with specific culture conditions can promote differentiation into a variety of tissues, including bone, cartilage, fat, and muscle.[1] As a result of these favorable characteristics, MSCs are considered ideal cells for tissue engineering purposes.

Recent studies have demonstrated significant advances in tissue engineering. Numerous groups have shown that complex tissues can be synthesized *in vitro* or with the use of bioreactors.[2–5] MSCs seeded on synthetic or naturally occurring matrices have been used to produce precisely shaped constructs to replace diseased or damaged tissues.[4,6–8] Although these findings are exciting, several factors limit this technique from becoming routine in clinical practice. One of the biggest obstacles to the use of tissue-engineered constructs in reconstruction of tissue defects is the lengthy culture and manufacturing periods required by conventional techniques. For instance, the synthesis of a tissue-engineered bone construct usually requires a 6–12 week culture and seeding period.[9–11]

These long construction times are not oncologically safe for rapidly growing malignancies. Similarly, long culture periods are a significant drawback to the use of tissue-engineered constructs for traumatic defects, as they would require prolonged open wound care and convalescence. Further, tissue-engineered constructs produced *in vitro* lack a vascular supply and are thereby limited in size and prone to infection or re-absorption.

The use of exogenous growth factors may be a means by which tissue-engineered construct synthesis and vascularization can be accelerated. Bone morphogenetic proteins (*BMPs*) may be a method by which osteogenesis can be enhanced in a tissue-engineered bone construct since these growth factors are known to promote osseous repair in endochondral and membranous bones.[12–14] *BMPs* are critical for successful fracture repair and bone development, and exogenous delivery of *BMP* can induce bone formation in critical-sized bone defects.[15,16] Thus, genetic manipulation of cell-seeded MSC constructs with *BMP* may represent a viable method to accelerate or augment bone deposition.

Division of Plastic and Reconstructive Surgery, Department of Surgery, Memorial Sloan-Kettering Cancer Center, New York, New York.

Similarly, delivery of angiogenic growth factors, such as vascular endothelial growth factor (*VEGF*), may be a means by which vascular ingrowth can be augmented since these molecules regulate angiogenesis. Further, several studies have shown that angiogenesis and osteogenesis are synergistic.[17–20] Thus, genetic modification of cell seeded constructs with *VEGF* may augment vascular ingrowth and osteogenesis in a tissue-engineered construct, thereby accelerating construct synthesis and angiogenesis.

In the current study we hypothesized that increased expression of both *BMP2* and *VEGF-A* to a tissue-engineered construct seeded with MSCs would augment osteogenesis and angiogenesis. We focused on *VEGF-A* as this is the major proangiogenic isoform.[21] Interestingly, we found that codelivery of these growth factors requires optimization as *VEGF* potently inhibited BMP2 expression. Conversely, *BMP2* had little effect on *VEGF* expression. The inhibition of *BMP2* expression by *VEGF* occurred at the RNA level, and *VEGF* inhibited the expression of endogenous *BMP2* as well as adenovirally delivered *BMP2*. The latter finding suggests that *VEGF* inhibition occurs independently of the *BMP2* promoter since the adenoviral gene expression was driven by a constitutively active promoter. Taken together, our findings suggest that approaches utilizing concurrent delivery of growth factors require optimization of growth factor concentration. In addition, we present evidence for interaction between *VEGF* and *BMP* expression at the RNA level.

Materials and Methods

Isolation and culture expansion of bone marrow–derived MSCs

Bone marrow–derived MSCs from 2- to 5-day-old inbred Lewis rats (LEW/SsNHsd; Harlan, Indianapolis, IN) were used for the *in vitro* experiments and a green fluorescent protein (*GFP*) transgenic strain (LEW-Tg [EGFP] F455/Rrrc, Rat Resource and Research Center [RRRC], University of Missouri, Columbia, MO) were used for the *in vivo* experiments. MSCs were isolated using previously published techniques.[22] Briefly, the femur and tibia bone marrow was flushed using a 28-gauge needle and Iscoves modified Dulbecco medium (MDM) containing 2% fetal bovine serum (StemCell Technologies, Vancouver, BC, Canada). The collected bone marrow samples were centrifuged, resuspended, and plated in Mesencult medium (StemCell Technologies) containing 100 units/mL penicillin, 100 μg/mL streptomycin, and stimulatory supplements designed to optimally initiate and maintain MSC proliferation. Cells were cultured at 37°C in a humidified, 5% CO_2 atmosphere. Early passage cells (i.e., no more than three passages) were used for all experiments. Potential for differentiation into fat, bone, and cartilage in the differentiation medium specific for each lineage was analyzed to confirm MSC isolation (data not shown). In addition, consistent with previous reports on MSC antigen expression, flow cytometric cell sorting (FACs) analysis demonstrated that more than 85% of the isolated cells expressed CD 105, 29, and Sca-1, whereas over 98% of the cells were negative for CD45 and CD34 (not shown).

Adenovirus synthesis and purification

Recombinant, replication-deficient adenoviruses expressing the bacterial *LacZ* gene (AdV-LacZ) and human *BMP2* (AdV-BMP2) (both from Vector Biolabs, Philadelphia, PA), and mouse *VEGF-A* (AdV-VEGF) (Cell Biolabs, San Diego, CA) were amplified in 293 cells. The LacZ virus was used as our control virus based on our previous studies utilizing adenoviruses.[23] Importantly, all adenoviruses were built on the same backbone, and expression was driven by the constitutively active cytomegalovirus (CMV) promoter. Adenovirus purification was performed using the ViraBind Adenovirus Purification Kit (Cell Biolabs).

Calculation of the number of plaque-forming units (PFU) in the viral stock was preformed using QuickTiter Adenovirus Titer Immunoassay Kit (Cell Biolabs) using the manufacturer's methods. Briefly, 5×10^5 293 cells were seeded in 12-well plates and incubated for 1 h. A 10-fold serial dilution of the viral stock was then added to the wells, and after 2 days of incubation, immunostaining with the provided Hexon antibody was preformed. Positively stained cells were then counted using a hemocytometer and compared to wells infected with a positive viral control of known concentration.

Transfection of MSCs

To optimize the expression of both *VEGF* and *BMP2*, MSCs were counted, plated, and infected (1 h after plating) with various ratios of recombinant adenovirus to a total multiplicity of infection (MOI) of 100 PFU/cell (Table 1). We administered the *BMP2* virus in a 9:1, 3:1, or 1:1 ratio together with either the *VEGF* virus or the control LacZ virus. Thus, for the 9:1 ratio we infected the MSCs using a combination of 90 PFU/cell of the *BMP2* virus together with 10 PFU/cell of the *VEGF* or LacZ virus. Similarly, the 3:1 ratio corresponded to 75 PFU/cell of the *BMP2* virus together with 25 PFU/cell of the *VEGF* or *LacZ* virus, and so on. This was based on our preliminary studies demonstrating that a 1:1 concentration of *BMP2* and *VEGF* virus (i.e., 50 PFU BMP2 together with 50 PFU VEGF) resulted in minimal *BMP2* expression. Analysis of gene expression, protein production, and mRNA stability was performed 48 h after viral infection ($n = 3$/group).

To evaluate the paracrine interactions between *BMP2* and *VEGF*, MSCs were transfected separately with *BMP2* or *VEGF* at an MOI of 100 PFU/cell. Twelve hours after trans-

Table 1. Treatment Groups for Cotransfection/Coculture Experiment

Group	*Treatment (MOI of adenovirus)*
1	Vehicle
2	100 (AdV-BMP2)
3	100 (AdV-VEGFa)
4	50 (AdV-BMP2) + 50 (AdV-VEGFa)
5	50 (AdV-BMP2) + 50 (AdV-LacZ)
6	50 (AdV-VEGFa) + 50 (AdV-LacZ)
7	90 (AdV-BMP2) + 10 (AdV-LacZ)
8	90 (AdV-BMP2) + 10 (AdV-VEGFa)
9	75 (AdV-BMP2) + 25 (AdV-VEGFa)
10	75 (AdV-BMP2) + 25 (AdV-LacZ)
11[a]	100 (AdV-BMP2) + 100 (AdV-VEGFa)

[a]Group 11 is plated as a coculture of cells from group 2 and group 3, about 12 h after transfection.

BMP2, bone morphogenetic protein 2; VEGF, vascular endothelial growth factor; MOI, multiplicity of infection.

fection, cells were trypsinized, counted, and re-plated. Thus, in the resulting coculture, half of the cells had been transfected to overexpress *BMP2* (MOI 100) and half of the cells had been transfected to overexpress *VEGF* (MOI 100). Thirty-six hours after re-plating, cocultured cells and controls were analyzed for gene and protein expression.

Proliferation assay

To determine if cotransfection of MSCs altered the rate of proliferation of these cells, MSCs were plated at a density of 2×10^3 cells in 96-well plates (BD, Franklin Lakes, NJ). The following day, cells were transfected with a total MOI of 100 PFU/cell using varying ratios of *BMP2*, *VEGF*, or *LacZ* virus. The relative cell number was then assessed every other day for 8 days using the CellTiter96 Aqueous Assay (Promega, Madison, WI) according to the manufacturer's instructions ($n=5$/group). This assay relies on the mitochondrial conversion of 3-(4,5-dimethylthiazol-2-yl)-5-(3-carboxymethoxyphenyl)-2-(sulfophenyl)-2H-tetrazolium) (MTS) to formazan since this reaction has been shown to be directly proportional to the number of living cells in the culture.

Real-time semiquantitative reverse transcription polymerase chain reaction

For real-time polymerase chain reaction (PCR), virally transfected cells were harvested and total cellular RNA was isolated using RNeasy kit (Qiagen, Valencia, CA) according to the manufacturer's protocol. RNA quantity and quality of the purified samples was analyzed using a NanoDrop ND 1000 Spectrophotometer (NanoDrop Technologies, Wilmington, DE). About 1 μg of total RNA from each sample was reverse transcribed using TaqMan Reverse Transcription Reagents Kit (Applied Biosystems, Foster City, CA).

Quantitative real-time (qRT)-PCR primers and probes for *VEGF*, *BMP2*, *RUNX-2*, *18s rRNA*, and *Hexon* (Applied Biosystems) were used to perform PCR (50 cycles; $n=3$/group) on an ABI Prism 7900HT using 2× TaqMan Universal PCR Master Mix (Applied Biosystems). The *Hexon* primers correspond to virus-specific genes independent of the recombinant gene inserted in the viral genome. Thus, quantification of the *Hexon* gene expression was used to confirm our viral quantification. Relative quantization was then performed and normalized for ribosomal 18S RNA and viral-specific *Hexon* RNA. The candidate genes and primers used for quantitative real-time PCR are listed in Table 2.

Table 2. Quantitative RT-Polymerase Chain Reaction Gene Expression Primer/Probe Information

Gene	*Catalog no. or primer/probe details*
Vascular endothelial growth factor A (*VEGFa*)	Mm00437304_m1
Bone morphogenetic protein 2 (*BMP2*)	Mm01340178_m1
Human adenovirus C serotype 5 Hexon Gene (*Hexon*)	HEXON LEFT: atggacaacgtcaacccatt HEXON RIGHT: ctccgtcaacccttaggtca OLIGO: 6FAM-cgagtggaacttcaggaagg
Eukaryotic 18s rRNA (18s rRNA)	Hs99999901_s1
RUNX-2	Mm00501584_m1

Enzyme-linked immunosorbent assay

Virally transfected cells, plated at a density of 5×10^4 per well ($n=3$/group) in 24-well plates, were harvested 48 h after transfection. The expression of *BMP2* and *VEGF-A* protein in the culture medium was determined using enzyme-linked immunosorbent assay (ELISA) kits (R&D Systems, Minneapolis, MN) as per the manufacturer's instructions. Minimal detectable dose was 3.0 pg/mL for *VEGF* and 11 pg/mL for *BMP2*.

BMP2 expression after exogenous supplementation of VEGF

To exclude the possibility that viral interaction between the *VEGF* and *BMP2* adenoviruses was responsible for the inhibition of *BMP2* expression, the effect of recombinant mouse *VEGF-A* on MSCs transfected with BMP2 adenovirus was evaluated. MSCs were transfected with 100 PFU/cell of the BMP2 adenovirus and then exposed to the medium supplemented to a final concentration of 10 or 50 ng/mL recombinant human *VEGF* (rhVEGF) (R&D Systems) for 48 h. *BMP2* production was then determined through the ELISA measurement (R&D Systems Quanitkine Kit) as described above.

The effects of rhVEGF on MSC differentiation into bone

To determine the effect of *VEGF* protein on MSC differentiation down the osteogenic pathway, MSCs were grown in the bone differentiation medium and exposed to recombinant mouse *VEGF*. Briefly, 1×10^5 MSCs were grown on six-well plates in a nondifferentiating medium for 2 days. The medium was then changed to a bone differentiation medium (composed of the Mesencult stem cell medium supplemented with 5 mM β-glycerophosphate, 10^{-8} M dexamethasone, and 0.28 mM ascorbic acid [all from Sigma, St. Louis, MO]) with 10 ng/mL rhVEGF, 50 ng/mL rhVEGF (R&D Systems), or no *VEGF*. RNA was harvested after 12 h of incubation. All experiments were carried out in triplicate. quantitative real time-PCR was performed as described above to determine gene expression of early bone differentiation marker *RUNX-2* (Applied Biosystems). Some cells were left in the bone differentiation medium for 21 days and analyzed for calcium deposition using von Kossa staining: cells were fixed in 4% paraformaldehyde, and then exposed to 5% silver nitrate and ultraviolet light for 45 min. After serial rinses in distilled water, 5% sodium thiosulfate (in H_2O) was added for 5 min. After two rinses with distilled water, nuclear fast red (Sigma) was added for 5 min. Culture plates were then and digitally imaged at 100×.

Transcriptional and translational effects of VEGF on BMP mRNA and protein

To determine if the inhibition of *BMP2* by *VEGF* occurred as a result of changes in transcription or translation in MSCs, these processes were inhibited using RNA-polymerase II inhibitor actinomycin-D or the protein synthesis inhibitor cycloheximide. For evaluating mRNA stability and degradation,

experimental cells were transfected with AdV-BMP2 at an MOI of 50 PFU/cell and the next day exposed to the medium containing 5 ng/mL actinomycin-D (Sigma), with or without 10 ng/mL *VEGF* (R&D Systems). For evaluating posttranslational inhibitory mechanisms, cells were transfected with the combination of either AdV-BMP2 and AdV-VEGF or AdV-BMP2 and AdV-LacZ at a 1:1 ratio and at that time exposed to the medium containing 10 ng/mL cycloheximide (Sigma). RNA was harvested hourly for 3 h after actinomycin-D and 6 h after cycloheximide supplementation. *BMP2* mRNA was measured using semiquantitative real time PCR as described above. Slopes were extrapolated by linear regression.

In vivo *implantation and scaffold preparation*

To determine whether dual transfection of MSCs with the *BMP* and *VEGF* viruses had any *in vivo* effects, MSCs were seeded on collagen scaffolds and implanted in the epigastric fat pad in rats. Three-dimensional collagen composite scaffolds (BD Biosciences, Bedford, MA) composed of bovine collagen I and III (diameter 5 mm, height 3 mm, average pore size 100–200 μm) were used. Before rehydration, a 1 mm central circular pore was created in the scaffolds using a 1 mm hole punch. Scaffolds were then hydrated and seeded with 5×10^4 *GFP*-positive MSCs and cultured for 1 h, followed by a second cell seeding with 5×10^5 cells for an additional hour. Constructs were then kept at the air–medium interface using a 12 mm cell culture inserts (Millipore, Billerica, MA) and cultured for 12 days. Two days before *in vivo* transfer, cell-seeded scaffolds were transfected with various ratios of *BMP2*, *VEGF*, or *LacZ* adenoviruses with an MOI of 100 PFU/cell.

After transfection, cell-seeded collagen scaffolds were implanted in syngeneic non-*GFP* rats (LEW/SsNHsd; Harlan). Animals were anesthetized and a 2–3 cm incision was made along the femoral vessels. The superficial inferior epigastric artery and vein were located and carefully freed from the groin fat pad. The pedicle was ligated and pulled through the center of the perforated collagen scaffold. The construct was then covered by the fat pad of the groin and the incision was closed. The procedures were approved by the Animal Care Committee of the Memorial Sloan-Kettering Cancer Center.

Animal imaging and tissue processing

Four weeks after implantation, the animals were anesthetized with isoflurane, secured, and examined with the CT component of the X-SPEC dual-modality SPECT/CT system (Gamma Medica Ideas, Northridge, CA). Samples were harvested for histology the following day. The constructs were fixed using 4% paraformaldehyde and decalcified in 0.5 M ethylenediaminetetraacetic acid (Sigma) for 48 h. Constructs were then split in half, where one half was used for frozen tissue processing and the other half paraffin embedded, sectioned at 5 μm intervals, and stained with hematoxylin and eosin using standard techniques. The samples intended for cryosectioning were transferred to 30% sucrose in phosphate-buffered saline for 24 h at 4°C and then embedded in optimal cutting temperature and sectioned at 15 μm intervals.

Sections were imaged using a (Zeiss Axioplan 2 microscope, Jena, Germany) in bright field or with GFP excitation and emission filters set for 470 and 525 nm, respectively. To assess for autofluorescence, filters for tetramethylrhodamine isothiocyanate (TRITC) set at excitation 535 and emission 620 were used. Samples were digitally captured using a linked Zeiss AxioCam MRm and the Axiovision software overlaying images for GFP and TRITC. Specificity of the GFP signal was further assured using a (Leica TCS SP2 AOBS, Wetzlar, Germany) confocal microscope determining the fluorescent spectra of the sample.

Statistical analysis

Statistical analysis was conducted using InStat (San Diego, CA) software. Due to the limited number of samples, nonparametric tests were used to analyze statistical significant

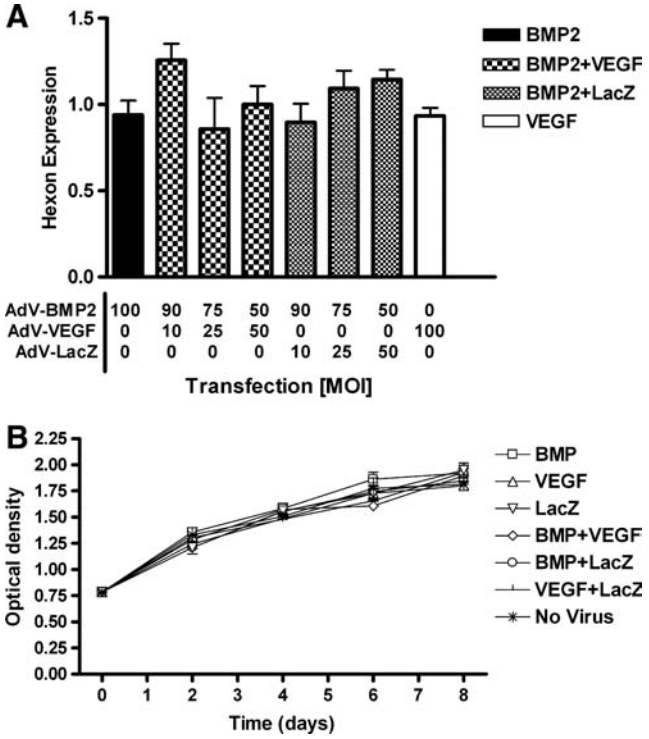

FIG. 1. Adenoviral transfection without proliferative alterations or signs of toxicity. Adenoviral vectors carrying the gene for *BMP2*, *VEGF*, or *LacZ* were used to transfect bone marrow–derived rat MSCs. Combinations of the genes were introduced to the cells at a total MOI of 100 PFU/cell. (**A**) Relative quantities of adenovirus Hexon mRNA expression were then analyzed ($n=3$/group) and normalized by concurrent analysis of ribosomal *18S RNA*. Similar levels of adenovirus-specific *Hexon mRNA* expression suggest that the viral load and efficacy of transfection were similar in all groups. Values represent mean ± SD of replicates ($n=3$). (**B**) Alterations in growth was assessed at various time-points using the 3-(4,5-diamethylthiazol-2-yl)-5-(3-carboxymethoxyphenyl)-2-(4-sulfophenyl)-2H-tetrazolium) (MTS) assay and compared to nontransfected controls. The growth curves were similar in all groups, and at the final day of the assay, no significant difference in optical density (proportional to cell number) was found between the groups. Labels in the graph represent the introduced genes and the corresponding viral MOI. Values represent mean ± SD of replicates ($n=5$/group). *BMP2*, bone morphogenetic protein 2; *VEGF*, vascular endothelial growth factor; MOI, multiplicity of infection; PFU, plaque forming units; SD, standard deviation; MSCs, mesenchymal stem cells.

differences between groups. Kruskal–Wallis test was used for multigroup comparisons and Mann–Whitney test was used for comparison between two groups. Data are presented as mean ± standard deviation, with $p < 0.05$ considered significant.

Results

Cotransfected AdV-VEGF decreases BMP2 expression in MSCs

To evaluate potential interactions between *BMP2* and *VEGF* when both genes were simultaneously introduced into MSCs, cells were transfected with varying ratio's of *BMP2* and *VEGF* or *BMP2* and *LacZ*. No proliferative alterations or signs of toxicity could be detected as a result of the transfection. In addition, the viral load with each virus type appeared to be similar based on the expression of viral-specific *Hexon* gene as evaluated by rtPCR (Fig. 1A). The growth curves were similar in all groups; at the final day of the assay, no significant difference in relative cell number was found between the groups (Fig. 1B).

When we analyzed the production of *BMP2* protein after dual transfection with *LacZ*, we noted an asymptotic decrease in *BMP2* expression, as expected, when this gene was

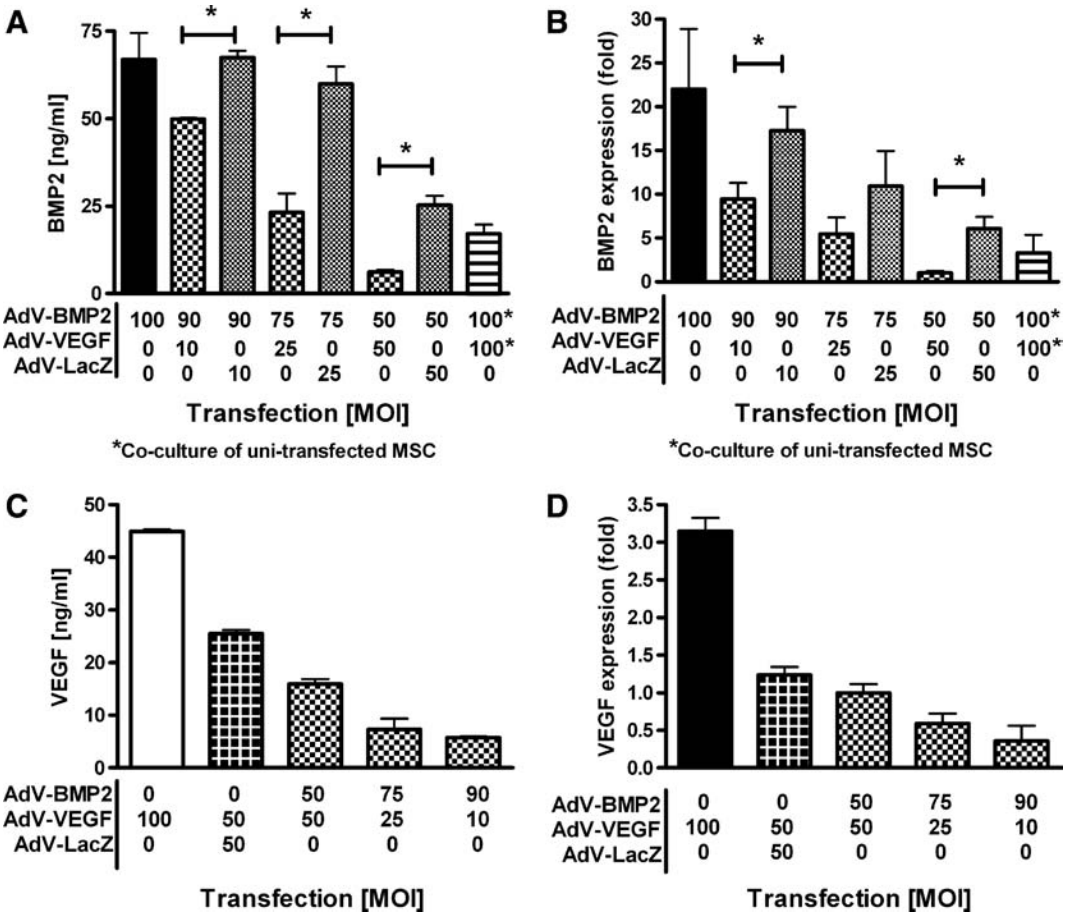

FIG. 2. Cotransfection of AdV-VEGF decreases BMP2 expression. Adenoviral vectors carrying the gene for BMP2, VEGF, or LacZ were used to transfect bone marrow–derived rat MSCs. Combinations of the genes were introduced to the cells at a total MOI of 100 PFU/cell. (**A**) When BMP2 was coexpressed with LacZ in various ratios, while keeping the total viral load constant, the mRNA expression varied according to the AdV-BMP2 MOI. When the same ratios were applied to the AdV-BMP2 and AdV-VEGF cotransfection, however, the BMP2 expression was drastically reduced, demonstrating an exponential distribution that seemed correlated to the AdV- BMP2:VEGF ratio rather than the AdV-BMP2 MOI alone. One group was plated as a coculture composed of cells, separately transfected with AdV-BMP2 and AdV-VEGF. The total number of cells as well as the total viral load and average AdV-BMP2 vector per cell was equal to the groups dually transfected with BMP2 (MOI 50) + VEGF (MOI 50) or BMP2 (MOI 50) + LacZ (MOI 50). The levels of BMP2 were approximately three times higher in cultures composed of separately transfected cells compared to cells dually transfected with AdV-BMP2 and AdV-VEGF. Separately transfected but cocultured cells expressed, however, less BMP2 compared to cells dually transfected with AdV-BMP2 and AdV-LacZ. (**B**) When the levels of BMP2 and VEGF were measured in the cell medium through real time PCR, the general patterns corresponded to the ELISA results and demonstrated that the phenomenon occurs at the mRNA level. (**C, D**) The expression of VEGF correlated to the AdV-VEGF MOI, relatively independent of any AdV-BMP2 or AdV-LacZ cotransfection, when evaluated with ELISA and rtPCR. Relative quantities of RNA were obtained by normalization against ribosomal 18S RNA as well as viral-specific Hexon RNA to weigh in any variations in viral transfection between groups. Labels in the graph represent the introduced genes and the corresponding viral MOI. Values represent mean ± SD of replicates ($n = 3$). ELISA, enzyme-linked immunosorbent assay; PCR, polymerase chain reaction.

codelivered with *LacZ*. The asymptotic decrease was expected because the ratios with which we codelivered *BMP2* were not linear (i.e., 9:1, 3:1, and 1:1). Thus, transfection of *BMP2* independently at an MOI of 100 PFU/cell resulted in the production of nearly 70 ng/mL of *BMP2* protein (Fig. 2A). This value decreased only slightly when a 9:1 (i.e., 90 PFU/cell of *BMP2* virus) or 3:1 (i.e., 75 PFU/cell of the *BMP2* virus) ratio of the *BMP2-LacZ* virus was used. Delivery of the *BMP2* virus in a 1:1 ratio (i.e., 50 PFU/cell of *BMP2* virus plus 50 PFU/cell of the LacZ virus) with the *LacZ* virus resulted in an approximately 2.5-fold decrease in *BMP2* production, reflecting the 50% decrease in *BMP* adenovirus used.

In contrast, codelivery of *BMP2* and *VEGF* demonstrated an exponential decrease in *BMP2* protein production. This decrease suggests that *VEGF* delivery inhibits production of *BMP2*. We noted a marked inhibition of *BMP2* expression in all combinations of *BMP2:VEGF*. For example, when we delivered *BMP2* in a 1:1 ratio with *VEGF* (i.e., 50 PFU/cell of *BMP2* virus plus 50 PFU/cell VEGF virus), *BMP2* protein expression was nearly completely abolished (>10-fold decrease). The difference between *BMP2* expression when transfection was performed in conjunction with AdV-LacZ was significantly higher at all concentrations when compared with cotransfections with AdV-VEGF ($p < 0.05$ at each ratio).

The inhibition of *BMP2* expression by *VEGF* occurs at the transcriptional level as demonstrated in Figure 2B. Thus, when *BMP2* was coexpressed with *LacZ* in various ratios but with constant total viral load, *BMP2* mRNA expression, similar to our protein data, varied according to the AdV-BMP2 MOI in an asymptotic manner. In contrast, when *BMP2* was codelivered with *VEGF*, the expression of *BMP2* was drastically reduced, demonstrating an exponential change that was correlated with the ratio of the AdV-*BMP2:VEGF* ratio rather than the AdV-BMP2 MOI alone.

Interestingly, we found that dual transfection of cells with *BMP2* and *VEGF* did not inhibit *VEGF* expression (Fig. 2C, D) to the same extent. Thus, unlike *BMP2* mRNA expression, there was no significant difference in *VEGF* expression when comparing cells transfected with *VEGF:BMP2* and those transfected with *VEGF:LacZ*. In these cases, as would be expected in a case without significant interaction, *VEGF* protein and mRNA expression correlated with the number of *VEGF* adenovirus PFU. These findings indirectly support our hypothesis that BMP2 expression is inhibited by *VEGF* rather than a virus-specific effect.

AdV-VEGF–mediated BMP2 inhibition occurs through autocrine as well as paracrine mechanisms

To assess whether the effect of *VEGF* expression on *BMP2* production was autocrine or paracrine in nature, MSCs were separately transfected with AdV-BMP2 or AdV-VEGF at an MOI 100 PFU/cell, then mixed, and cultured together. The resulting coculture was then analyzed for *BMP2* protein and mRNA expression and compared with cotransfected cells. The total number of cells as well as the total viral load and average AdV-BMP2 vector per cell was equal between the coculture group and groups dually transfected with *BMP2*

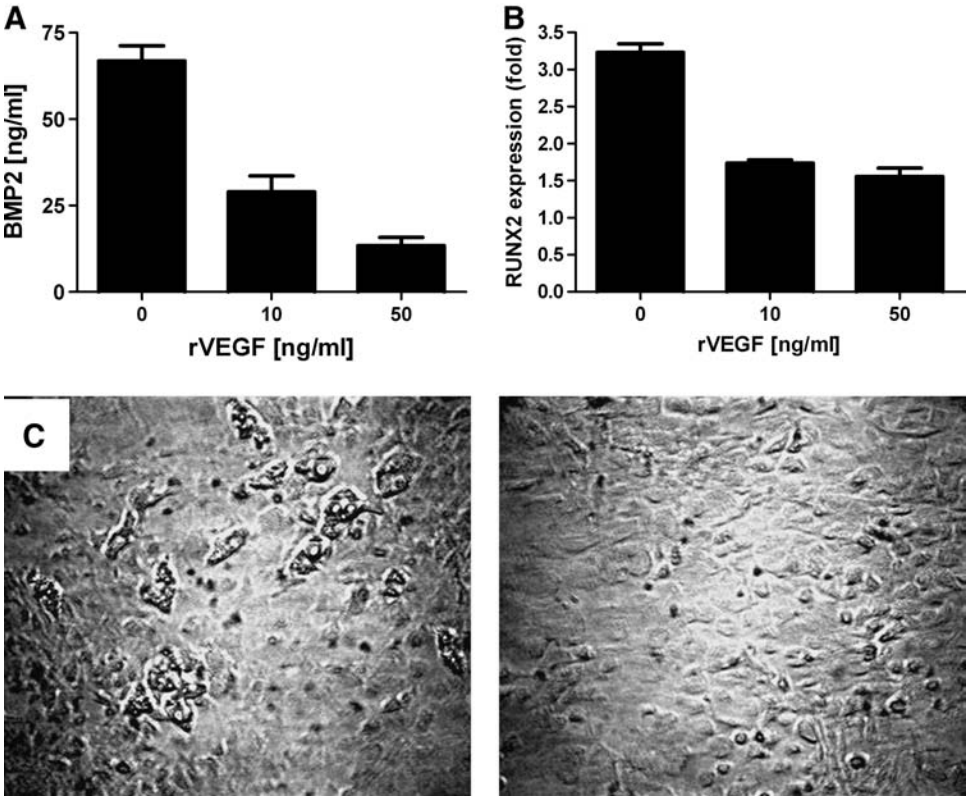

FIG. 3. Adenoviral-mediated BMP2 overexpression and MSC differentiation can be suppressed by exogenous VEGF. (**A**) Bone marrow–derived rat MSCs transfected with Adv-BMP2 at an MOI of 100 PFU/cell were exposed to the medium supplemented with 10 or 50 ng/mL recombinant VEGF protein. After 48 h, cultures were analyzed with ELISA and showed a dose-dependant decrease in BMP2 production dependent on the VEGF concentration. BMP2 production decreased fivefold when VEGF was supplemented to a concentration of 50 ng/mL, indicating that exogenous VEGF is a potent inhibitor of BMP2 expression in MSCs. (**B**) MSCs were cultured in the differentiation medium and assessed for expression of early bone differentiation marker RUNX-2. At 12 h RUNX-2 expression was markedly reduced in cells exposed to recombinant VEGF. (**C**) While positive staining for calcium deposits was found in cell cultures grown for 21 days in the differentiation medium without rhVEGF (left), little signs of bone formation were present in cultures grown under the same conditions but with VEGF-supplement (right).

(MOI 50) + *VEGF* (MOI 50) or *BMP2* (MOI 50) + *LacZ* (*MOI* 50). In both ELISA (Fig. 2A) and rtPCR assays (Fig. 2B), the levels of BMP2 were approximately three times higher in cultures composed of separately transfected cells compared with cells dually transfected with AdV-BMP2 and AdV-VEGF. Separately transfected but cocultured cells expressed, however, 30–50% less *BMP2* compared with cells dually transfected with AdV-BMP2 and AdV-LacZ. These findings suggest that inhibition of *BMP2* by *VEGF* occurs as a result of both autocrine and paracrine mechanisms. Similar to our cotransfection experiments, we noted no inhibition of *VEGF* expression when cells were cocultured with *BMP2*-expressing MSCs (data not shown).

Suppressed BMP2 expression and MSC differentiation by exogenous VEGF

The hypothesis that *VEGF* inhibits *BMP2* expression is supported by the finding that recombinant *VEGF* protein at physiologically relevant doses inhibits endogenous *BMP2* expression in a dose-dependent manner (Fig. 3A). Decreased expression of *BMP2* is further reflected by a similar expression pattern for *RUNX-2*, a critical transcription factor regulating early osteoblastic differentiation (Fig. 3B). Further, MSCs grown in the bone differentiation medium showed greater potential for bone nodule formation in the absence of *VEGF* when compared with cells grown under the same conditions with *VEGF* supplement (Fig. 3C). Collectively, these studies suggest that *VEGF* inhibits *BMP2* expression and decreases osteoblastic differentiation of MSCs.

BMP2 inhibition occurs at the transcriptional level

In an effort to delineate the molecular mechanisms by which *VEGF* inhibits *BMP2* expression, we utilized the transcription and translation inhibitors actinomycin-D and cycloheximide, respectively. The finding that VEGF can inhibit the expression of both endogenous and forced expression of *BMP2* is interesting and has mechanistic relevance, since in the latter case *BMP2* expression is driven by the constitutively active *CMV* promoter. This implies that the inhibitory effects of *VEGF* on *BMP2* are independent of the endogenous *BMP2* promoter. Therefore, to evaluate mRNA stability, we inhibited RNA transcription using actinomycin-D. A time course of *BMP2* transcript expression after exposure to antitranscriptional agent actinomycin-D with or without supplemented *VEGF* demonstrated a similar rate of *BMP2* transcript degradation (slope -0.4872 ± 0.03695 vs. -0.5059 ± 0.1170) (Fig. 4A). This finding implies that VEGF reduces *BMP2* expression by a method other than transcriptional degradation. When cells were cotransfected with *BMP2* and *VEGF* adenoviruses, the addition of cycloheximide caused no increase in *BMP2* production (Fig. 4B), indicating that translation of an inhibitory protein is not necessary for inhibition of *BMP2* expression by *VEGF*.

VEGF-mediated BMP2 inhibition impairs bone formation in vivo

To evaluate the effects of *BMP2* and *VEGF* codelivery on *in vivo* bone formation, we cultured *GFP*-positive MSCs on a three-dimensional collagen scaffold for 12 days and then double transfected with Adv-BMP2 and Adv-VEGF or Adv-

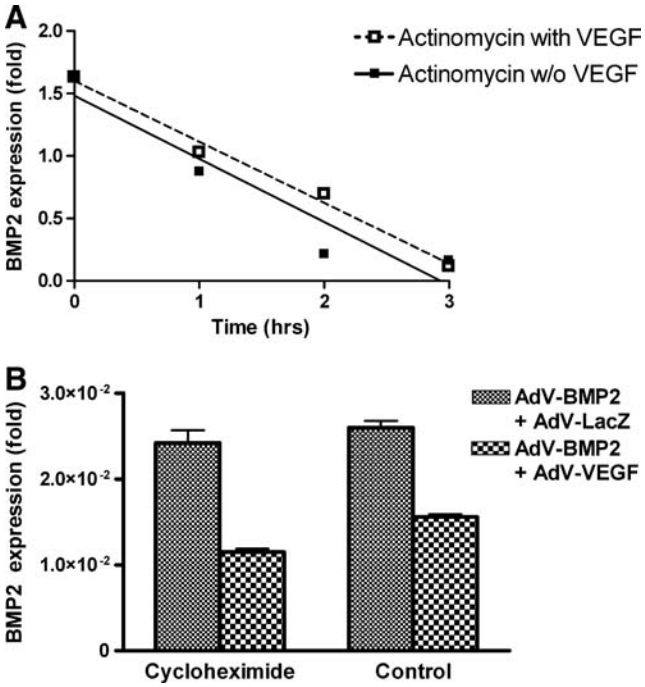

FIG. 4. BMP2 inhibition occurs at the transcriptional level. To determine if the inhibition of BMP2 by VEGF occurred as a result of changes in transcription or translation, these processes were inhibited using RNA-polymerase II inhibitor actinomycin-D or the protein synthesis inhibitor cycloheximide. (**A**) Rat MSCs were transfected with AdV-BMP2 at an MOI of 50 PFU/cell and exposed to the medium containing 5 ng/mL actinomycin-D, with or without 10 ng/mL VEGF. A time course of BMP2 transcript expression demonstrated a similar rate of BMP2 transcript degradation (slope -0.4872 ± 0.03695 vs. -0.5059 ± 0.1170), implying that VEGF reduces BMP2 expression by a method other than transcriptional degradation. (**B**) MSCs were transfected with the combination of either AdV-BMP2 and AdV-VEGF or AdV-BMP2 and AdV-LacZ at a 1:1 ratio and then exposed to the medium containing 10 ng/mL cycloheximide. Six hours after cycloheximide supplementation analysis with rtPCR showed no increase in BMP2 expression, indicating that protein translation is not necessary for inhibition of BMP2 expression by VEGF. Values represent mean ± SD of replicates ($n = 3$).

BMP2 and Adv-LacZ viruses at a 1:1 ratio to a total MOI of 100 PFU/cell. Other constructs were transfected with *BMP2* virus alone at an MOI of 100 PFU/cell. Scaffolds were then implanted in the superficial inferior epigastric fat pad and analyzed 3 weeks later. Consistent with our *in vitro* findings, we found that combination of Adv-BMP2:Adv-VEGF in a 1:1 ratio completely prevented bone formation (Fig. 5A). Further, no *GFP*-positive cells could be identified in histological sections, suggesting that the implanted cells/constructs were completely absorbed. This finding suggests that a threshold or lower limit of *BMP2* expression is necessary for survival and incorporation of implanted MSCs. In contrast, constructs transfected with only AdV-BMP2 or cotransfected with AdV-BMP2 and AdV-LacZ produced bone (Fig. 5B, C). Numerous *GFP*-positive osteocytes could easily be identified in the bone matrix, demonstrating that implanted MSCs not only delivered *BMP2* but also directly contributed to bone formation (Fig. 5D). These *in vivo* findings confirm our *in vitro*

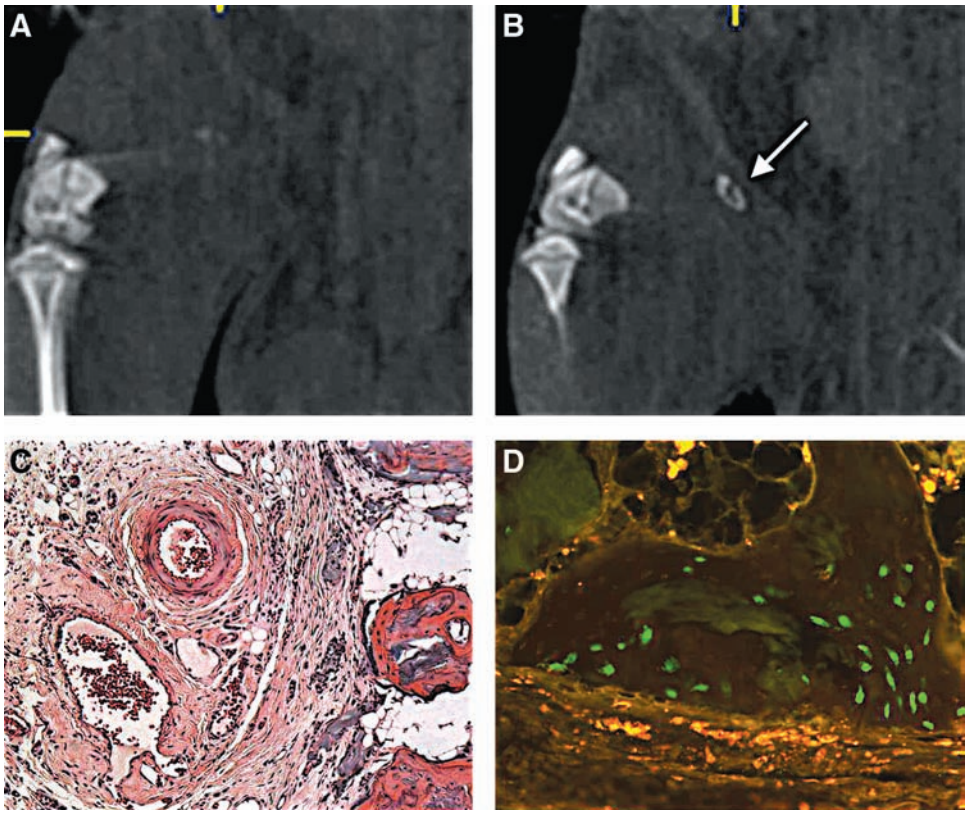

FIG. 5. VEGF-mediated BMP2 inhibition impairs bone formation *in vivo*. Bone marrow–derived MSCs from green fluorescent transgenic rats were seeded on collagen scaffolds and transfected with adenoviral vectors carrying the gene for BMP2, VEGF, or LacZ. Combinations of the genes were introduced to the cells at a 1:1 ratio with a total MOI of 100 PFU/cell. Constructs were then implanted in the groin of syngeneic green fluorescent protein–negative rats, and the superficial epigastric artery and vein were incorporated into the implant. While constructs transfected with AdV-BMP2 and AdV-VEGF formed little or no bone (**A**), implants transfected with AdV-BMP2 and AdV-LacZ were completely or in part replaced by bone (arrow) (**B**) as shown in the microcomputed tomography images. Decalcified sections of the AdV-BMP2:LacZ implants showed formation of cancellous bone surrounding the epigastric pedicle (arrow) (**C**). Donor cells expressing green fluorescent protein could be found within the osseous tissue (**D**). Color images available online at www.liebertonline.com/ten.

results that VEGF inhibits *BMP2* expression and bone differentiation in MSCs.

Discussion

In this study we demonstrate that *VEGF* can inhibit the expression of *BMP2* and subsequent osteoblastic differentiation in MSCs *in vitro* and *in vivo*. We found that this inhibition occurs with both endogenously produced BMP2 as well as after transfection of cells with a *BMP2* adenovirus under the regulation of a constitutively active CMV promoter. The significance of our findings is that tissue engineering techniques seeking to maximize osteogenesis and angiogenesis have to be carefully optimized since these processes are intimately linked. Further, as *VEGF* and *BMP2* have been shown to be highly conserved, these findings have immediate therapeutic implications.[24–27]

The validity of our conclusions is supported by a number of studies. For instance, Li and colleagues recently found that coexpression of *VEGF* and *BMP4* in pluripotent cells drastically reduced the cells bone-forming potential.[28] Similar to our results the impaired calcification was obvious even when a high *BMP*-to-*VEGF* viral ratio (5:1) was used. Unlike our findings, however, Li and colleagues did not see a direct reduction in BMP expression but correlated the incomplete ossification to impaired differentiation and proliferation. This discrepancy is perhaps due to the different cell types and viral vectors used in the two studies. Both our conclusions are, however, supported by the study of Geiger *et al.*, who demonstrated that elevated levels of *VEGF* impaired healing of a critical-sized defect.[29] While implantation of unmanipulated MSCs increased bone formation, implantation of MSCs genetically engineered to produce *VEGF* failed to heal the defect. Similarly, Patel *et al.* failed to show significant *VEGF* contribution to osteogenesis and healing of a critical bone defect. In fact, defects treated with *VEGF* demonstrated significant impairment of osteogenesis as compared to *BMP2*-treated controls.[30] Further, other studies have shown that proliferating chondrocytes in early osteogenesis secrete angiogenic inhibitors and that inhibition of *VEGF* signaling leads to a dose-dependent increase in epiphyseal growth plate area.[31–33]

It has also been suggested that *VEGF* expression is suppressed in some settings to prevent MSC differentiation toward an endothelial lineage.[19,34] Our results, however, suggest that *VEGF* directly prevents osteogenic commitment by inhibiting *BMP2* expression. These findings, together with those of studies demonstrating that mineralization of the endochondral mold and osteoblast infiltration is closely related to increased *VEGF* expression and vascular ingrowth, suggest that the balance of bone formation and vascular invasion is critical. Consequently, it is probable that bone-forming and angiogenic growth factors are involved in feedback mechanisms and that neither constant over or under expression of *VEGF* during *de novo* osteogenesis is beneficial.[17,18,20,35]

Peng *et al.*[18,19] also studied the interaction between BMP4 and *VEGF* on bone formation and concluded that VEGF acted

synergistically with *BMP4* to produce bone both ectopically and in bone defects. This study was performed using retroviral vectors on muscle-derived stem cells, similarly to Li and colleagues's[28] study, but the cells were separately transfected and mixed together in varying ratios. Interestingly, when a ratio of 5:1 was used, unlike Li and colleagues's results, bone formation was augmented rather than impaired. However, when lower ratios were used, similar to our and Li and colleagues's results, bone formation was inhibited, and Peng *et al*. concluded in consistence with our findings that the *BMP:VEGF* ratio is critical for bone formation.

The slight inconsistency between Li and colleagues's and Peng *et al*.'s findings could perhaps be explained by the fact that Peng *et al*. used separately transfected cells. Our results indicate that *VEGF* inhibition is more pronounced in co-transfected cells compared with separately transfected but cocultured cells. Peng *et al*. hypothesized that inhibition of bone formation in the setting of high *VEGF* levels was due to differentiation of stem cells along the endothelial cell lineage rather than osteoblastic cell lineage. The authors did not, unlike our study, evaluate the expression levels of *BMP* at the various ratios of *BMP:VEGF* transfection. Our results suggest that the impaired differentiation and ossification is due to specific down regulation of BMP (either endogenous or driven by viral vectors).

We demonstrate that *VEGF* inhibits *BMP2* expression and that this inhibition occurs at the mRNA level. This conclusion is supported by the finding that even when we inhibited mRNA translation with cycloheximide, *BMP2* mRNA expression remained unaffected. The finding that *VEGF* can inhibit expression of both endogenous and adenovirally delivered *BMP2* under the control of the constitutively active CMV promoter suggests that this inhibition is independent of the promoter region of *BMP2*. Thus, it is possible that inhibition at the level of transcription can occur through other means including miRNA or posttranscriptional processing. Further, the *VEGF* downstream pathway is extremely complex, and is possible that it is a downstream effector molecule that directly contributes to *BMP2* inhibition. While we have excluded the possibility of *VEGF*-induced translation of an effector molecule as the cause of *BMP2* inhibition, *VEGF* activity may be miRNA dependent and may represent a mechanism for our findings.[36] These possibilities require further analysis.

It is possible that some of our observations may be virus specific; however, several lines of evidence argue against this possibility. For example, it may be theorized that the observed differences in gene expression could be due simply to differences in viral delivery and quantification. Alternatively, there may be differences in viral adhesion or cellular uptake. However, these possibilities are unlikely to explain our findings since we show that the expression of the viral-specific Hexon gene was similar in all groups and that correction of gene expression for Hexon expression did not result in significant changes in the observed outcomes. Further, all viral constructs were synthesized using the same adenovirus capsid, and the expression of all genes was regulated by the same CMV promoter. Finally, suppressed expression of *BMP2* was also demonstrated in unmanipulated MSC exposed to recombinant *VEGF*. Taken together, these findings strongly suggest that the observed inhibition is not a viral-specific phenomenon.

In conclusion, we have shown that *VEGF* can inhibit *BMP2* expression at the mRNA level. Codelivery of *BMP2* and *VEGF* for tissue engineering purposes or to heal bone defects therefore requires careful optimization and precise delivery of growth factors for maximal bone formation using MSCs.

Acknowledgments

The authors gratefully acknowledge financial support from the Swedish Foundation for Plastic Surgery Research, Knut & Alice Wallenbergs Foundation, Perssons Foundation and The Swedish Society of Medicine.

The authors gratefully acknowledge financial support from the Plastic Surgery Educational Foundation in the form of National Endowment for Plastic Surgery Award.

Technical services provided by the MSKCC Small-Animal Imaging Core Facility, supported in part by the National Institutes of Health (NIH) Small-Animal Imaging Research Program (SAIRP) Grant No. **R24 CA83084** and NIH Center Grant No. **P30 CA08748**, are gratefully acknowledged.

Disclosure Statement

No competing financial interests exist.

References

1. Pittenger, M.F., Mackay, A.M., Beck, S.C., Jaiswal, R.K., Douglas, R., Mosca, J.D., Moorman, M.A., Simonetti, D.W., Craig, S., and Marshak, D.R. Multilineage potential of adult human mesenchymal stem cells. Science **284,** 143, 1999.
2. Huss, F.R., and Kratz, G. Mammary epithelial cell and adipocyte co-culture in a 3-D matrix: the first step towards tissue-engineered human breast tissue. Cells Tissues Organs **169,** 361, 2001.
3. Baker, B.M., and Mauck, R.L. The effect of nanofiber alignment on the maturation of engineered meniscus constructs. Biomaterials **28,** 1967, 2007.
4. Hoerstrup, S.P., Kadner, A., Melnitchouk, S., Trojan, A., Eid, K., Tracy, J., Sodian, R., Visjager, J.F., Kolb, S.A., Grunenfelder, J., Zund, G., and Turina, M.I. Tissue engineering of functional trileaflet heart valves from human marrow stromal cells. Circulation **106,** I143, 2002.
5. Yang, D., Guo, T., Nie, C., and Morris, S.F. Tissue-engineered blood vessel graft produced by self-derived cells and allogenic acellular matrix: a functional performance and histologic study. Ann Plast Surg **62,** 297, 2009.
6. Alhadlaq, A., and Mao, J.J. Tissue-engineered osteochondral constructs in the shape of an articular condyle. J Bone Joint Surg Am **87,** 936, 2005.
7. Liu, P., Deng, Z., Han, S., Liu, T., Wen, N., Lu, W., Geng, X., Huang, S., and Jin, Y. Tissue-engineered skin containing mesenchymal stem cells improves burn wounds. Artif Organs **32,** 925, 2008.
8. Yamasaki, T., Deie, M., Shinomiya, R., Yasunaga, Y., Yanada, S., and Ochi, M. Transplantation of meniscus regenerated by tissue engineering with a scaffold derived from a rat meniscus and mesenchymal stromal cells derived from rat bone marrow. Artif Organs **32,** 519, 2008.
9. Wu, B., Zheng, Q., Guo, X., Wu, Y., Wang, Y., and Cui, F. Preparation and ectopic osteogenesis *in vivo* of scaffold based on mineralized recombinant human-like collagen loaded with synthetic BMP-2-derived peptide. Biomed Mater **3,** 44111, 2008.
10. Oliveira, S.M., Amaral, I.F., Barbosa, M.A., and Teixeira, C.C. Engineering endochondral bone: *in vitro* studies. Tissue Eng Part A **15,** 625, 2009.

11. Oda, M., Kuroda, S., Konda, H., and Kasugai, S. Hydroxyapatite fiber material with BMP-2 gene induces ectopic bone formation. J Biomed Mater Res B Appl Biomater **90,** 101, 2009.
12. Lee, D.H., Park, B.J., Lee, M.S., Lee, J.W., Kim, J.K., Yang, H.C., and Park, J.C. Chemotactic migration of human mesenchymal stem cells and MC3T3-E1 osteoblast-like cells induced by COS-7 cell line expressing rhBMP-7. Tissue Eng **12,** 1577, 2006.
13. Minamide, A., Tamaki, T., Kawakami, M., Hashizume, H., Yoshida, M., and Sakata, R. Experimental spinal fusion using sintered bovine bone coated with type I collagen and recombinant human bone morphogenetic protein-2. Spine **24,** 1863–1870; discussion 71–72, 1999.
14. Sheehan, J.P., Sheehan, J.M., Seeherman, H., Quigg, M., and Helm, G.A. The safety and utility of recombinant human bone morphogenetic protein-2 for cranial procedures in a nonhuman primate model. J Neurosurg **98,** 125, 2003.
15. Nilsson, O.S., Urist, M.R., Dawson, E.G., Schmalzried, T.P., and Finerman, G.A. Bone repair induced by bone morphogenetic protein in ulnar defects in dogs. J Bone Joint Surg Br **68,** 635, 1986.
16. Peterson, B., Zhang, J., Iglesias, R., Kabo, M., Hedrick, M., Benhaim, P., and Lieberman, J.R. Healing of critically sized femoral defects, using genetically modified mesenchymal stem cells from human adipose tissue. Tissue Eng **11,** 120, 2005.
17. Maes, C., Carmeliet, P., Moermans, K., Stockmans, I., Smets, N., Collen, D., Bouillon, R., and Carmeliet, G. Impaired angiogenesis and endochondral bone formation in mice lacking the vascular endothelial growth factor isoforms VEGF164 and VEGF188. Mech Dev **111,** 61, 2002.
18. Peng, H., Usas, A., Olshanski, A., Ho, A.M., Gearhart, B., Cooper, G.M., and Huard, J. VEGF improves, whereas sFlt1 inhibits, BMP2-induced bone formation and bone healing through modulation of angiogenesis. J Bone Miner Res **20,** 2017, 2005.
19. Peng, H., Wright, V., Usas, A., Gearhart, B., Shen, H.C., Cummins, J., and Huard, J. Synergistic enhancement of bone formation and healing by stem cell-expressed VEGF and bone morphogenetic protein-4. J Clin Invest **110,** 751, 2002.
20. Zelzer, E., and Olsen, B.R. Multiple roles of vascular endothelial growth factor (VEGF) in skeletal development, growth, and repair. Curr Top Dev Biol **65,** 169, 2005.
21. Lohela, M., Bry, M., Tammela, T., and Alitalo, K. VEGFs and receptors involved in angiogenesis versus lymphangiogenesis. Curr Opin Cell Biol **21,** 154, 2009.
22. Okuyama, H., Krishnamachary, B., Zhou, Y.F., Nagasawa, H., Bosch-Marce, M., and Semenza, G.L. Expression of vascular endothelial growth factor receptor 1 in bone marrow-derived mesenchymal cells is dependent on hypoxia-inducible factor 1. J Biol Chem **281,** 15554, 2006.
23. Mehrara, B.J., Saadeh, P.B., Steinbrech, D.S., Dudziak, M., Spector, J.A., Greenwald, J.A., Gittes, G.K., and Longaker, M.T. Adenovirus-mediated gene therapy of osteoblasts *in vitro* and *in vivo*. J Bone Miner Res **14,** 1290, 1999.
24. Feng, J.Q., Harris, M.A., Ghosh-Choudhury, N., Feng, M., Mundy, G.R., and Harris, S.E. Structure and sequence of mouse bone morphogenetic protein-2 gene (BMP-2): comparison of the structures and promoter regions of BMP-2 and BMP-4 genes. Biochim Biophys Acta **1218,** 221, 1994.
25. Clauss, M., Gerlach, M., Gerlach, H., Brett, J., Wang, F., Familletti, P.C., Pan, Y.C., Olander, J.V., Connolly, D.T., and Stern, D. Vascular permeability factor: a tumor-derived polypeptide that induces endothelial cell and monocyte procoagulant activity, and promotes monocyte migration. J Exp Med **172,** 1535, 1990.
26. Senger, D.R., Connolly, D.T., Van de Water, L., Feder, J., and Dvorak, H.F. Purification and NH2-terminal amino acid sequence of guinea pig tumor-secreted vascular permeability factor. Cancer Res **50,** 1774, 1990.
27. Senger, D.R., Perruzzi, C.A., Feder, J., and Dvorak, H.F. A highly conserved vascular permeability factor secreted by a variety of human and rodent tumor cell lines. Cancer Res **46,** 5629, 1986.
28. Li, G., Corsi-Payne, K., Zheng, B., Usas, A., Peng, H., and Huard, J. The dose of growth factors influences the synergistic effect of vascular endothelial growth factor on bone morphogenetic protein 4–induced ectopic bone formation. Tissue Eng Part A **15,** 2123, 2009.
29. Geiger, F., Lorenz, H., Xu, W., Szalay, K., Kasten, P., Claes, L., Augat, P., and Richter, W. VEGF producing bone marrow stromal cells (BMSC) enhance vascularization and resorption of a natural coral bone substitute. Bone **41,** 516, 2007.
30. Patel, Z.S., Young, S., Tabata, Y., Jansen, J.A., Wong, M.E., and Mikos, A.G. Dual delivery of an angiogenic and an osteogenic growth factor for bone regeneration in a critical size defect model. Bone **43,** 931, 2008.
31. Hayami, T., Funaki, H., Yaoeda, K., Mitui, K., Yamagiwa, H., Tokunaga, K., Hatano, H., Kondo, J., Hiraki, Y., Yamamoto, T., Duong le, T., and Endo, N. Expression of the cartilage derived anti-angiogenic factor chondromodulin-I decreases in the early stage of experimental osteoarthritis. J Rheumatol **30,** 2207, 2003.
32. Moses, M.A., Sudhalter, J., and Langer, R. Identification of an inhibitor of neovascularization from cartilage. Science **248,** 1408, 1990.
33. Wedge, S.R., Ogilvie, D.J., Dukes, M., Kendrew, J., Chester, R., Jackson, J.A., Boffey, S.J., Valentine, P.J., Curwen, J.O., Musgrove, H.L., Graham, G.A., Hughes, G.D., Thomas, A.P., Stokes, E.S., Curry, B., Richmond, G.H., Wadsworth, P.F., Bigley, A.L., and Hennequin, L.F. ZD6474 inhibits vascular endothelial growth factor signaling, angiogenesis, and tumor growth following oral administration. Cancer Res **62,** 4645, 2002.
34. Oswald, J., Boxberger, S., Jorgensen, B., Feldmann, S., Ehninger, G., Bornhauser, M., and Werner, C. Mesenchymal stem cells can be differentiated into endothelial cells *in vitro*. Stem Cells **22,** 377, 2004.
35. Gerber, H.P., Vu, T.H., Ryan, A.M., Kowalski, J., Werb, Z., and Ferrara, N. VEGF couples hypertrophic cartilage remodeling, ossification and angiogenesis during endochondral bone formation. Nat Med **5,** 623, 1999.
36. Kuhnert, F., Mancuso, M.R., Hampton, J., Stankunas, K., Asano, T., Chen, C.Z., and Kuo, C.J. Attribution of vascular phenotypes of the murine Egfl7 locus to the microRNA miR-126. Development **135,** 3989, 2008.

Address correspondence to:
Babak J. Mehrara, M.D., FACS
1275 York Ave.
Room MRI 1005
New York, NY 10065

E-mail: mehrarab@mskcc.org

Received: June 24, 2009
Accepted: September 14, 2009
Online Publication Date: October 28, 2009